

# Color-Multiplexing-Based Fluorescent Test Paper: Dosage-Sensitive Visualization of Arsenic(III) with Discernable Scale as Low as 5 ppb

Yujie Zhou,<sup>†,#</sup> Xiaoyan Huang,<sup>†,#</sup> Cui Liu,<sup>‡</sup> Ruilong Zhang,<sup>‡,§</sup> Xiaoling Gu,<sup>†</sup> Guijian Guan,<sup>‡</sup> Changlong Jiang,<sup>‡</sup> Liying Zhang,<sup>†</sup> Shuhu Du,<sup>\*,†</sup> Bianhua Liu,<sup>‡,§</sup> Ming-Yong Han,<sup>‡</sup> and Zhongping Zhang<sup>\*,†,§,||</sup>

<sup>†</sup>School of Pharmacy, Nanjing Medical University, Nanjing, Jiangsu 211166, China

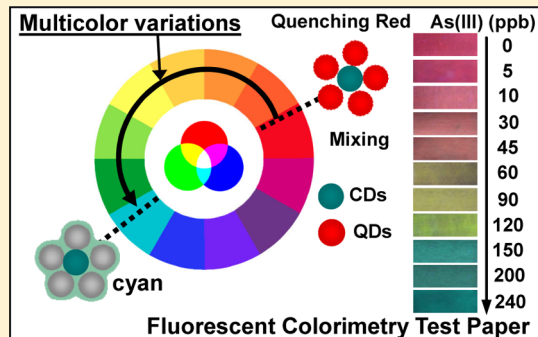
<sup>‡</sup>CAS Center for Excellence in Nanoscience, Institute of Intelligent Machines, Chinese Academy of Sciences, Hefei, Anhui 230031, China

<sup>§</sup>School of Chemistry and Chemical Engineering, Anhui University, Hefei, Anhui 230601, China

<sup>||</sup>State Key Laboratory of Transducer Technology, Chinese Academy of Sciences, Hefei, Anhui 230031, China

## Supporting Information

**ABSTRACT:** Fluorescent colorimetry test papers are promising for the assays of environments, medicines, and foods by the observation of the naked eye on the variations of fluorescence brightness and color. Unlike dye-absorption-based pH test paper, however, the fluorescent test papers with wide color-emissive variations with target dosages for accurate quantification remain unsuccessful even if the multicolorful fluorescent probes are used. Here, we report the dosage-sensitive fluorescent colorimetry test paper with a very wide/consecutive “from red to cyan” response to the presence and amount of arsenic ions, As(III). Red quantum dots (QDs) were modified with glutathione and dithiothreitol to obtain the supersensitivity to As(III) by the quenching of red fluorescence through the formation of dispersive QDs aggregates. A small amount of cyan carbon dots (CDs) with spectral blue-green components as the photostable internal standard were mixed into the QDs solution to produce a composited red fluorescence. Upon the addition of As(III) into the sensory solution, the fluorescence color could gradually be reversed from red to cyan with a detection limit of 1.7 ppb As(III). When the sensory solution was printed onto a piece of filter paper, surprisingly a serial of color evolution from peach to pink to orange to khaki to yellowish to yellow-green to final cyan with the addition of As(III) was displayed and clearly discerned the dosage scale as low as 5 ppb. The methodology reported here opens a novel pathway toward the real applications of fluorescent test papers.



Quantitative analysis of target species has been extensively performed by using conventional laboratory instruments, which are unsuitable for on-site assays as they are cumbersome and expensive and also require the complex pretreatments and professional operation by well-trained personnel. Therefore, there is an urgent demand to develop a fast, inexpensive, and portable strategy for the on-site detection in environments, medicines, and foods, which has always been attracting considerable efforts in the construction of new miniature chemical sensors. With high sensitivity and simplification, fluorescence-based sensors are most widely studied because of a wide range of available materials including fluorescent dyes,<sup>1</sup> quantum dots (QDs),<sup>2,3</sup> graphene oxide,<sup>4</sup> and carbon dots (CDs).<sup>5,6</sup> It is very critical to design a recognition element linkage on fluorescent probe for the productions of fluorescent “turn-off”, “turn-on”, or “ratiometric” responses.<sup>7,8</sup> Fluorescent sensors exhibit various potential applications in the sensitive detection of metal ions,<sup>9</sup> pesticides,<sup>10</sup> explosives,<sup>11,12</sup> and biological molecules.<sup>13–15</sup> To

achieve this, unfortunately, they still need to largely depend on fluorescent instruments such as a fine fluorescent spectrometer or confocal microscope.

However, fluorescent sensors possess another unparalleled advantage, that is, their visualization capability for the determination of analyte with the naked eye by the aid of a simple ultraviolet (UV) lamp. Owing to the classical success of pH test paper, the fluorescent test papers have been widely explored by assembling or printing the fluorescent probes onto a piece of paper-based substrates for the visual assays with low cost, easy operation, and portable feasibility, for example, QDs paper for the detection of explosives,<sup>16</sup> CDs paper for the assay of heavy metal ions,<sup>17</sup> graphene oxide paper for the identification of peptide/protein and DNA,<sup>18</sup> and upconversion nanoparticle paper for the determination of pesticides.<sup>19</sup> In

Received: March 30, 2016

Accepted: May 27, 2016

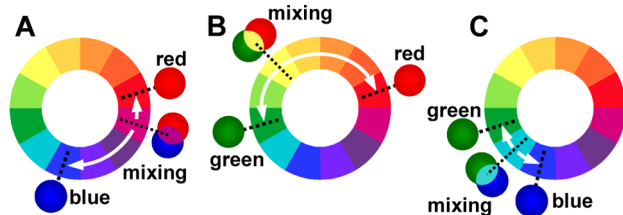
Published: May 27, 2016

general, a single-colorful fluorescent probe only can display the change of fluorescence brightness by either “turn on” or “turn off” with analytes, greatly limiting their quantitative capability. An accurate/visual quantification mainly depends on the color variations rather than only brightness, because our eye is more sensitive to colors. However, the use of multicolorful fluorescent probes toward the wide color variations with target dosages remains unsuccessful, because they lead to the formation of intermediate composite color, compressing the range of color variation. Nowadays, the fluorescent test paper with pH test paper-like performances remains a daunting challenge.

In this paper, we develop a fluorescent colorimetry strategy for a dosage-sensitive detection of As(III) species as an example with the clear color visualization on paper by the use of ratiometric fluorescent red/cyan probes. As(III) is highly toxic and there are about 140 million people exposed to high arsenic-contaminated water worldwide.<sup>20</sup> The current analysis of As(III) mainly depends on atomic absorption spectrometry<sup>21</sup> and inductively coupled plasma mass spectrometry.<sup>22</sup>

The wide color-varying test papers are usually involved in the joint employments of multicolorful probes. Scheme 1 illustrates

**Scheme 1. Red-Green-Blue (RGB) Chromaticity Analysis on the Ranges of Color Variation When the Typical Dual-Color Probes Are Coexisting in One System: (A) Red + Blue, (B) Red + Green, and (C) Green + Blue<sup>a</sup>**



<sup>a</sup>The arrows indicate the ranges of color variation.

the three typical situations on the ranges of color variation when the two probes among red-green-blue colors are used in one system. The mixture of red and blue probes in the ratio of 1:1 in fluorescent intensity leads to a purple, and thus the maximal range of color variations is either “from purple to red” or “from purple to blue” (Scheme 1A). That is to say, the wider range from “from red to blue” or “from blue to red” will not be achieved. Alternatively, the mixture of red and green probes leads to a yellow, and the range of color variations is only “from yellow to red” or “from yellow to green”. Similarly, if green is mixed with blue, the maximal range of color variations is only “from cyan to green” or “from cyan to blue”. The chromaticity analysis suggests that the 1:1 mixing of dual-color probes greatly compresses the range of color change due to the formation of intermediate composite colors.

In the present work, we propose a novel strategy to achieve a wide color variations from red to cyan by the use of red and cyan probes. As shown in Figure 1A, cyan CDs and red CdTe QDs are mixed and the ratio of emission intensity of cyan to red is adjusted to 1:5, which still displays a red to avoid the formation of an intermediate color. Here, the cyan of CDs is a mixing color of green and blue with chromaticity proportion of 2:1 (Figure S1). Thus, the CDs + QDs system is a mixture of red-green-blue with a chromaticity proportion of 10:2:1, offering the possibility of rich color variations. Finally, if the

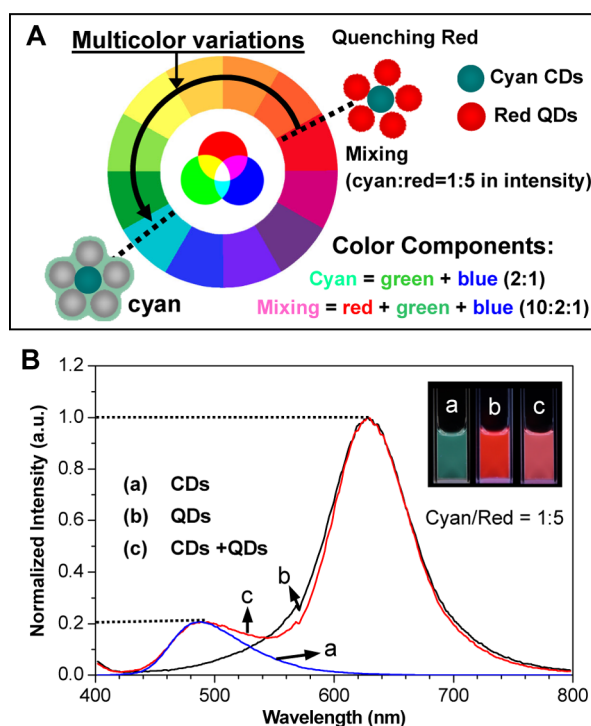


**Figure 1.** (A) Proposed strategy to achieve the wide range of color variations from red to cyan by the use of dual-color probes. (B) Fluorescent spectra of CDs and GSH/DTT-modified CdTe QDs and the mixing CDs/QDs at the excitation of 350 nm (the inset photos were taken under 365 nm UV lamp).

red fluorescence of QDs is gradually quenched by analytes, the percentages of red-green-blue colors continuously change to expand the range of color variations from red to cyan (Figure 1A). The premises for the visual effects are that red QDs must be supersensitive to analyte with quenching fluorescence, and cyan CDs as an internal standard are highly photostable.

Cyan CDs were synthesized using *m*-phenylenediamine as starting material by the hydrothermal method<sup>23</sup> (see the experimental details in the Supporting Information). The as-prepared CDs were about 7 nm in size by TEM examination (Figure S2) and had excellent aqueous solubility due to the presence of  $-NH_2$  groups at their surfaces (Figure S3). The reduced glutathione (GSH) modified CdTe QDs were prepared in the aqueous phase by the classical method,<sup>24</sup> in which GSH ligands greatly enhanced the aqueous solubility of QDs. The GSH-QDs were further modified with dithiothreitol (DTT) by replacing GSH ligands in part, playing a role of sensory ligand to bind As(III). GSH/DTT-QDs were characterized by high-resolution TEM, infrared spectroscopy, energy-dispersive X-ray spectroscopy, and UV-visible spectroscopy (Figures S2–S5).

Furthermore, dynamic light scattering gave the hydrate particle sizes of  $\sim 15$  and 10 nm for CDs and GSH/DTT-QDs, respectively (Figure S6), which were much larger than the sizes themselves. Their zeta potentials were +1.87 and  $-6.86$  mV, respectively. These measurements reveal the excellent hydrophilicity of CDs and GSH/DTT-QDs.

The fluorescent spectrum of CDs exhibited an emission peak at 486 nm excited at 350 nm and a bright cyan fluorescence under the UV lamp (Figure 1B and the inset image). Moreover, the fluorescence of CDs was highly stable (Figure S7), satisfying the requirement of an internal standard in ratiometric

fluorescence. The fluorescent spectrum of GSH/DTT-QDs had an emission peak at 630 nm excited at 350 nm and displayed a bright red fluorescence under UV lamp (Figure 1B and the inset). As proposed in Figure 1A, when we mixed CDs and GSH/DTT-QDs and adjusted the ratio of fluorescent intensity (cyan to red) to 1:5, the mixing solution displayed peach color under UV lamp (the inset of Figure 1B) and the fluorescent spectra of mixture exhibited the two identical peaks at 486 and 630 nm and a full spectral coverage in the visual range from 400 to 800 nm.

Figure 2A illustrates the mechanism of As(III) detection using the ratiometric fluorescent GSH/DTT-QDs/CDs probes.

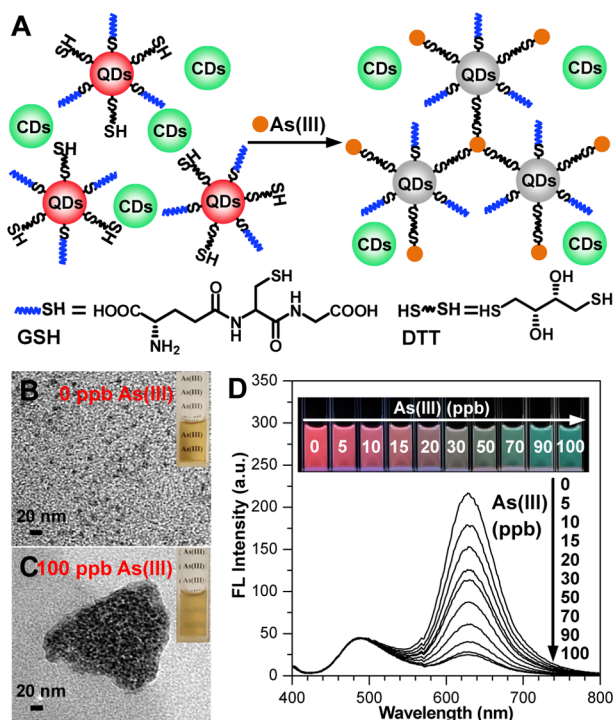


**Figure 2.** (A) Visualization mechanism of As(III) using GSH/DTT-QDs as fluorescent sensory probe and CDs as an internal standard probe. (B, C) TEM images of GSH/DTT-QDs before and after the addition of As(III) (the insets are the corresponding optical photos under daylight). (D) Fluorescent spectra of mixing GSH/DTT-QDs/CDs (20/10  $\mu\text{L}$  in 1.5 mL of Tris-HCl buffer, pH 7.4) with the addition of As(III). The inset photos show the evolution of corresponding colors under 365 nm UV lamp.

GSH ligand contains  $-\text{NH}_2$ ,  $-\text{COOH}$ , and  $-\text{SH}$  groups, in which  $-\text{SH}$  binds onto the Cd ion at the surface of QDs and the free  $-\text{NH}_2$  and  $-\text{COOH}$  greatly increase the water solubility of QDs. However, the GSH-QDs do not have the obvious fluorescent response to As(III) (Figure S8). Therefore, the further modification with DTT molecule with two  $-\text{SH}$  groups is done to result in numerous free  $-\text{SH}$  groups at the surface of QDs. It is well-known that As(III) has very strong binding affinity to DTT with a standard stability constant  $K$  of  $6.31 \times 10^{37}$  in the As(III)-DTT complex.<sup>25</sup> Upon the addition of As(III), the formed As-S bonds induce the aggregation of GSH/DTT-QDs to quench the red fluorescence of QDs.<sup>26–28</sup> In the presence of cyan CDs as an internal standard, the gradual quenching of red fluorescence will produce a consecutive color variation with the increase of the As(III) amount in the system.

The above mechanism was further confirmed by the TEM examinations. Before the addition of As(III), the GSH/DTT-QDs solution was light yellow and highly transparent to clearly see the “As(III)” on the white background (the inset photo in Figure 2B), and the TEM image revealed the high monodisperse state of QDs. With the addition of As(III), the solution became opaque due to the formation of small aggregates of QDs, as revealed by TEM in Figure 2C and Figure S9.

Figure 2D shows the evolution of fluorescent spectra of the mixture of CDs and GSH/DTT-QDs with the titration of As(III). The red fluorescence peak at 630 nm was gradually quenched, and the cyan fluorescence peak at 486 nm kept highly steady, which were completely identical to the cases of pure GSH/DTT-QDs and CDs, respectively (Figure S10). With the increase of As(III) up to 100 ppb, surprisingly, the intensity ratio of cyan to red was reversed from 1:5 to 1:0.5 due to the superquenching of red fluorescence by As(III). That is to say, the fluorescence of system was transformed from “strong red, weak cyan” into “strong cyan, weak red”, leading to a wide color variations with As(III) dosages as shown by the inset of Figure 2D. The detailed experiments revealed that the best visualization effect of color change could be obtained at the 1:5 ratio of cyan to red in fluorescent intensity (Figure S11).

The ratio of fluorescent intensities,  $\ln(I_{630}/I_{486})$ , showed a dosage-dependence with good linearity against As(III) concentrations in the range of 5–100 ppb with correlation coefficient  $R = 0.994$  (Figure S12). The detection limit ( $3\sigma$ ) was calculated to be 1.7 ppb. Moreover, we added different amounts of As(III) into tap water and lake water to test the reliability of this method. Table S1 showed that the recoveries of As(III) in tap water and lake water were in the range of 98.7–102.8% and 102.2–103.7%, respectively, determined by the linear relationship of ratiometric fluorescence. These data suggest that the mixing probes can efficiently work in tap water and lake water for the reliable detection of As(III).

In addition, the spectral selectivity was evaluated by the measurements of ratiometric fluorescence and the observations of fluorescence colors. When As(V),  $\text{Na}^+$ ,  $\text{K}^+$ ,  $\text{Ca}^{2+}$ ,  $\text{Co}^{2+}$ ,  $\text{Mg}^{2+}$ ,  $\text{Al}^{3+}$ ,  $\text{Ni}^{2+}$ ,  $\text{Mn}^{2+}$ ,  $\text{Cd}^{2+}$ ,  $\text{Zn}^{2+}$ ,  $\text{Pb}^{2+}$ , or  $\text{Hg}^{2+}$  was added into the mixing system, the ratio  $I_{630}/I_{486}$  of fluorescent spectra remained almost unchanged, meanwhile the fluorescence colors under UV lamp still displayed the original peach (Figure S13), suggesting an excellent selectivity to As(III). Although  $\text{Cu}^{2+}$  and  $\text{Fe}^{3+}$  ions perturbed the detection of As(III), the addition of  $\text{SCN}^-$  and  $\text{F}^-$  anions completely eliminated their interferences by the formations of complexes (Figure S14). The dynamics experiments evidenced that the fluorescent response to As(III) was completed in  $\sim 1$  min (Figure S15).

On the basis of above studies, we have further developed the fluorescent test paper of As(III) to confirm its dosage-sensitive ability for visual quantification with the wide and consecutive color variations. The mixture of CDs and GSH/DTT-QDs (1:5 in fluorescent intensity) as ink was jet-printed onto a piece of filter paper by the control of a computer (Figure S16).<sup>18</sup> The filter paper was nonfluorescent under 365 nm UV lamp to avoid the interference to visual colorimetry. The preparation procedure made the probes evenly stick to the matrix of paper fibers, overcoming their disassociations from paper upon contacting analyte solution (Figure S17).

When the aqueous solution of As(III) was evenly added onto a piece of  $3 \times 1 \text{ cm}^2$  test paper, the remarkable color changes with the dosages of As(III) were seen under UV lamp.

Interestingly, each dosage indicated in Figure 3A from 0 to 240 ppb corresponded an eye-discernible color from peach to pink

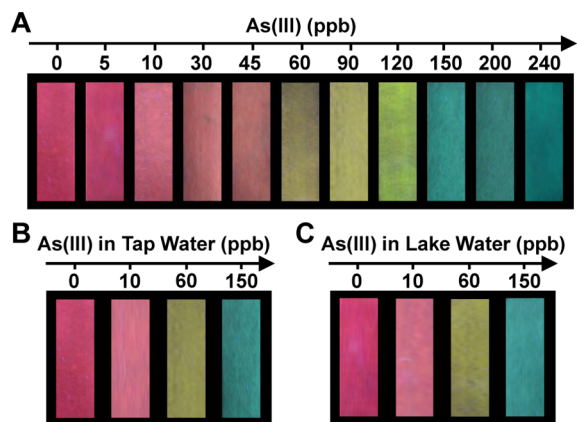


**Figure 3.** (A) Visualization of As(III) using the fluorescent test papers prepared by printing GSH/DTT-QDs/CDs ink on a piece of filter paper. (B, C) Visual detections of As(III) in tap water and lake water, respectively. The photos were taken under 365 nm UV lamp.

to orange to khaki to yellowish to yellow-green to final cyan, which was similar to pH test paper performance and was in a good agreement with our proposed mechanism. After As(III) solution permeated into the matrix of paper fibers, GSH/DTT-QDs were exfoliated from paper fibers to form the dispersive aggregates on paper, leading to the quenching of QDs fluorescence and thus the color changes. Moreover, it was seen that each chromaticity was highly uniform over a whole piece of test paper due to the homogeneous distribution of two probes there. Significantly, the red of the test paper at even 5 ppb As(III) was lighter than that at 0 ppb but deeper than that at 10 ppb, indicating the discernible dosage scale as low as 5 ppb, which was lower than 10 ppb As(III) in drinking water prescribed by the World Health Organization's guideline.

Furthermore, we spiked As(III) of 10, 60, and 150 ppb into tap water and lake water to validate the visual effect and accuracy of test paper. The displaying colors at the 10, 60, and 150 ppb As(III) in tap water (Figure 3B) were almost identical to those in lake water (Figure 3C), which were also accordant with the corresponding colors in Figure 3A. These confirm that the as-prepared test papers are actually applicable for the detections of As(III) in water samples.

In summary, we have proposed a general strategy to construct the wide-color-varying fluorescent test paper for the dosage-sensitive visualization assays like classical pH test paper. A wide range of consecutive color variations for the visual detection of As(III) in water has been achieved by three key points: (1) the use of cyan internal probe and sensory red probe; (2) the unequal-proportional mixing of the dual-color probes to avoid the formation of intermediate composite color; (3) the supersensitivity of designed red probe to As(III). On the basis of aggregation-induced sensitive mechanism, the superquenching of red fluorescence with As(III) resulted in the change of ratiometric fluorescence and thus a wide range of color variations with the dosage of As(III). Importantly, high-quality test papers were prepared by inkjet printing using the mixing fluorescent probe ink, and exhibited a dosage-sensitive color response with a discernible scale as low as 5 ppb As(III) with the observation of naked eye. The results reported here prospect a bright future of fluorescent colorimetry test papers

for the extensive applications in the assays of environments, medicines, and foods.

## ■ ASSOCIATED CONTENT

### 📄 Supporting Information

The Supporting Information is available free of charge on the ACS Publications website at DOI: 10.1021/acs.analchem.6b01248.

Experimental description, characterizations of CDs and QDs, preparation of fluorescent test paper, and supplementary figures and tables (PDF)

## ■ AUTHOR INFORMATION

### Corresponding Authors

\*E-mail: shuhudu@njmu.edu.cn.

\*E-mail: zpzhang@iim.ac.cn. Fax: (+86) 551-65591156.

### Author Contributions

\*Y.Z. and X.H. contributed equally to this work.

### Notes

The authors declare no competing financial interest.

## ■ ACKNOWLEDGMENTS

This work is supported by the National Basic Research Program of China (Grant 2015CB932002), China-Singapore Joint Project (Grant 2015DFG92510), Science and Technology Service Network Initiative of Chinese Academy of China (Grant KFJ-SW-STS-172), National Natural Science Foundation of China (Grants 21275075, 21335006, 21475135, 21375131, 21277145, and 21275145), and Natural Science Foundation of Anhui Province (Grant 1408085MKLS2).

## ■ REFERENCES

- (1) Li, K.; Xiang, Y.; Wang, X. Y.; Li, J.; Hu, R. R.; Tong, A. J.; Tang, B. Z. *J. Am. Chem. Soc.* **2014**, *136*, 1643–1649.
- (2) Gill, R.; Bahshi, L.; Freeman, R.; Willner, I. *Angew. Chem., Int. Ed.* **2008**, *47*, 1676–1679.
- (3) Kim, J. Y.; Voznyy, O.; Zhitomirsky, D.; Sargent, E. H. *Adv. Mater.* **2013**, *25*, 4986–5010.
- (4) Zhu, Z.; Tang, Z. W.; Phillips, J. A.; Yang, R. H.; Wang, H.; Tan, W. H. *J. Am. Chem. Soc.* **2008**, *130*, 10856–10857.
- (5) Ding, H.; Yu, S. B.; Wei, J. S.; Xiong, H. M. *ACS Nano* **2016**, *10*, 484–491.
- (6) Liu, J. H.; Cao, L.; LeCroy, G. E.; Wang, P.; Meziani, M. J.; Dong, Y. Y.; Liu, Y. F.; Luo, P. G.; Sun, Y. P. *ACS Appl. Mater. Interfaces* **2015**, *7*, 19439–19445.
- (7) Zhang, J. Y.; Guo, W. *Chem. Commun.* **2014**, *50*, 4214–4217.
- (8) Yao, J. L.; Zhang, K.; Zhu, H. J.; Ma, F.; Sun, M. T.; Yu, H.; Sun, J.; Wang, S. H. *Anal. Chem.* **2013**, *85*, 6461–6468.
- (9) Mei, Q. S.; Jiang, C. L.; Guan, G. J.; Zhang, K.; Liu, B. H.; Liu, R. Y.; Zhang, Z. P. *Chem. Commun.* **2012**, *48*, 7468–7470.
- (10) Zhang, K.; Mei, Q. S.; Guan, G. J.; Liu, B. H.; Wang, S. H.; Zhang, Z. P. *Anal. Chem.* **2010**, *82*, 9579–9586.
- (11) Goldman, E. R.; Medintz, I. L.; Whitley, J. L.; Hayhurst, A.; Clapp, A. R.; Uyeda, H. T.; Deschamps, J. R.; Lassman, M. E.; Mattoussi, H. *J. Am. Chem. Soc.* **2005**, *127*, 6744–6751.
- (12) Gao, D. M.; Wang, Z. Y.; Liu, B. H.; Ni, L.; Wu, M. H.; Zhang, Z. P. *Anal. Chem.* **2008**, *80*, 8545–8553.
- (13) Kong, H.; Lu, Y. X.; Wang, H.; Wen, F.; Zhang, S. C.; Zhang, X. R. *Anal. Chem.* **2012**, *84*, 4258–4261.
- (14) Yang, Z. G.; Cao, J. F.; He, Y. X.; Yang, J. H.; Kim, T.; Peng, X. J.; Kim, J. S. *Chem. Soc. Rev.* **2014**, *43*, 4563–4601.
- (15) Tan, C. L.; Yu, P.; Hu, Y. L.; Chen, J.; Huang, Y.; Cai, Y. Q.; Luo, Z. M.; Li, B.; Lu, Q. P.; Wang, L. H.; Liu, Z.; Zhang, H. *J. Am. Chem. Soc.* **2015**, *137*, 10430–10436.

- (16) Zhang, K.; Zhou, H. B.; Mei, Q. S.; Wang, S. H.; Guan, G. J.; Liu, R. Y.; Zhang, J.; Zhang, Z. P. *J. Am. Chem. Soc.* **2011**, *133*, 8424–8427.
- (17) Yuan, C.; Liu, B. H.; Liu, F.; Han, M. Y.; Zhang, Z. P. *Anal. Chem.* **2014**, *86*, 1123–1130.
- (18) Mei, Q. S.; Zhang, Z. P. *Angew. Chem., Int. Ed.* **2012**, *51*, 5602–5606.
- (19) Mei, Q. S.; Jing, H. R.; Li, Y.; Yisibashaer, W.; Chen, J.; Li, B. N.; Zhang, Y. *Biosens. Bioelectron.* **2016**, *75*, 427–432.
- (20) Cullen, W. R.; Reimer, K. J. *Chem. Rev.* **1989**, *89*, 713–764.
- (21) Pantuzzo, F. L.; Silva, J. C. J.; Ciminelli, V. S. T. *J. Hazard. Mater.* **2009**, *168*, 1636–1638.
- (22) Dufailly, V.; Noël, L.; Guérin, T. *Anal. Chim. Acta* **2008**, *611*, 134–142.
- (23) Jiang, K.; Sun, S.; Zhang, L.; Lu, Y.; Wu, A. G.; Cai, C. Z.; Lin, H. W. *Angew. Chem., Int. Ed.* **2015**, *54*, 5360–5363.
- (24) Zheng, Y. G.; Gao, S. J.; Ying, J. Y. *Adv. Mater.* **2007**, *19*, 376–380.
- (25) Kalluri, J. R.; Arbnesi, T.; Khan, S. A.; Neely, A.; Candice, P.; Varisli, B.; Washington, M.; McAfee, S.; Robinson, B.; Banerjee, S.; Singh, A. K.; Senapati, D.; Ray, P. C. *Angew. Chem., Int. Ed.* **2009**, *48*, 9668–9671.
- (26) Shen, P. F.; Xia, Y. S. *Anal. Chem.* **2014**, *86*, 5323–5329.
- (27) Wu, W. T.; Zhou, T.; Berliner, A.; Banerjee, P.; Zhou, S. Q. *Angew. Chem., Int. Ed.* **2010**, *49*, 6554–6558.
- (28) Wuister, S. F.; Donegá, C. D. M.; Meijerink, A. *J. Am. Chem. Soc.* **2004**, *126*, 10397–10402.